Watching the Brain as It (Un)Binds: Beta Synchronization Relates to Distractor–Response Binding

Bernhard Pastötter, Birte Moeller, and Christian Frings

Abstract

■ Human action control relies on event files, that is, short-term stimulus–response bindings that result from the integration of perception and action. The present EEG study examined oscillatory brain activities related to the integration and disintegration of event files in the distractor–response binding (DRB) task, which relies on a sequential prime–probe structure with orthogonal variation of distractor and response relations between prime and probe. Behavioral results indicated a DRB effect in RTs, which was moderated by the duration of the response-stimulus interval (RSI) between prime response and probe stimulus onset. Indeed, a DRB effect was observed for a short RSI of 500 msec but not for a longer RSI of 2000 msec, indicating disintegration of event files over time. EEG results revealed a positive correlation between individual DRB in the RSI-2000 condition and postmovement beta synchronization after both prime and probe responses. Beamformer analysis localized this correlation effect to the middle occipital gyrus, which also showed highest coherency with precentral and inferior parietal brain regions. Together, these findings suggest that postmovement beta synchronization is a marker of event file disintegration, with the left middle occipital gyrus being a hub region for stimulus–response bindings in the visual DRB task. ■

INTRODUCTION

Binding processes in the human brain are essential for perception, memory, and action. Cognitive representations of stimuli and events are stored in distributed neocortical networks. Therefore, binding processes are necessary to integrate these features into conjugate neural representations. The binding of stimulus features has been suggested to result in a hypothetical memory structure, the so-called "object file" (Kahneman, Treisman, & Gibbs, 1992), whereas the compound binding of stimulus and response features has been suggested to result in an "event file" (Hommel, 1998, 2004). Both (neural) long-term and short-term bindings exist in the brain. Long-term bindings that integrate features and distributed information in the brain related to semantic, episodic, and procedural long-term memories have been extensively studied in the neurosciences (Opitz, 2010; Fries, Fernandez, & Jensen, 2003). Thereby, different hub regions have been identified that orchestrate long-term bindings of semantic (the anterior temporal lobe; Patterson, Nestor, & Rogers, 2007), episodic (the hippocampus; Rolls, 1996), and procedural memories (the basal ganglia; Packard & Knowlton, 2002). To date, less is known about the neural signature of short-term bindings, that is, transient bindings in the time range of a few hundreds of milliseconds or seconds. These are typically assumed to reflect representations of associations in current (e.g., Fournier, Behmer, & Stubblefield, 2014; Stoet & Hommel, 1999) or recently executed action plans (e.g., Frings & Rothermund, 2011; Hommel, 1998), and are understood to play an important role in human action control (Frings et al., 2020; Henson, Eckstein, Waszak, Frings, & Horner, 2014).

Stimulus–Response Bindings

Evidence for short-term bindings (i.e., binding effects) can be observed in various paradigms that implement a trial structure including a sequence of two responses (see Frings et al., 2020). Two paradigms, explicitly designed to study short-lived stimulus–response bindings are the S1R1-S2R2 task, which addresses target–response binding, and the distractor–response binding (DRB) task. In the S1R1-S2R2 task (Hommel, 1998), an arbitrary response (e.g., a left-hand or right-hand key press; R1) is executed together with a prime stimulus (S1), without depending on any particular feature of S1. Shortly after the prime response, a probe stimulus (S2) is displayed and participants are instructed to respond to a specific feature of S2 (e.g., its color) by pressing the left or right key (R2). From prime to probe, stimulus feature and response identity are either repeated or alternated, with orthogonal manipulation of the two factors. The typical finding is faster and more accurate response repetitions (RRs) if the stimulus feature is repeated than if the stimulus feature is alternated, and faster and more accurate response changes (RCs) if the stimulus feature is alternated than if the stimulus feature is repeated, which can be described as partial repetition

University of Trier

Journal of Cognitive Neuroscience 33:8, pp. 1581–1594
https://doi.org/10.1162/jocn_a_01730

costs. The S1R1-S2R2 task is typically used to analyze bindings between target–features and responses. By contrast, the DRB task is typically used to analyze bindings between responses and additional response irrelevant stimuli (Frings, Rothermund, & Wentura, 2007). Here, the task is identical in the prime and the probe display: Targets (e.g., letters) are presented together with, oftentimes flanking, distractors (e.g., other letters). The participants' task is to respond to the target identities (e.g., via a left-hand or right-hand key press) and ignore the distractors. The typical finding is that RRs are faster and more accurate if distractor stimuli are repeated than if they change from prime to probe, whereas RCs are faster and more accurate if distractors change than if they are repeated. Statistically, the DRB effect is indicated by an interaction of response relation and stimulus relation. These partial repetition costs are referred to as behavioral DRB effects in RTs and accuracy in the following.

The widely accepted assumption is that responding to the target in the prime leads to integration of stimulus and response features in an event file (Hommel, 1998, 2004)—an internal representation of the stimulus–response compound. Event files have been described as a loose network of mostly binary bindings. Upon repetition of any feature that was integrated in the event file, other integrated features are retrieved, influencing responding (see Hommel, Müsseler, Aschersleben, & Prinz, 2001). Hence, in the DRB task, it is assumed that distractors are integrated with responses during the prime. Repetition of the same distractor during the probe then triggers retrieval of the (past) prime response. Such retrieval facilitates probe responding, if the same response is required as is retrieved. It leads to probe response impairment if retrieved and required responses differ. Notably, all paradigms, used to analyze binding effects, including the DRB task, separate two processes that are necessary for binding effects to emerge: feature *integration* in the prime (or $n - 1$) and *retrieval* because of feature repetition in the probe (or n; Frings et al., 2020).

Stimulus–response bindings as studied in the S1R1-S2R2 and the DRB task are short-lived. Frings (2011), for instance, varied the response-stimulus interval (RSI) between the prime response and probe onset in the DRB task between 500 or 2000 msec and demonstrated a DRB effect in RT if the RSI was 500 msec but not if the RSI was 2000 msec. Moeller, Pfister, Kunde, and Frings (2016) also showed that the DRB effect in RT was larger if the RSI was 500 msec than when it was 2000 msec, although the effect was significant in both conditions. Notably, in both of these studies, no significant influence of the RSI on the DRB effect in response accuracy was observed. Corroborating these findings, Hommel and Frings (2020) recently showed that partial repetition costs because of both target–response binding and DRBs decrease with increasing length of the RSI. Together, these findings indicate that stimulus–response bindings in the S1R1-S2R2 and the DRB task are short-lived in the time range of a few hundreds of milliseconds or seconds. The findings by Hommel and Frings (2020) further suggest that the disintegration of event files is best described by a decay function and that interference from intervening events in the RSI does not affect the disintegration.

Neural Correlates

Various studies examined the neural activities related to the retrieval of event files in stimulus–response binding tasks. For instance, with regard to target–response binding, an fMRI study by Kühn, Keizer, Colzato, Rombouts, and Hommel (2011), which used the S1R1-S2R2 task with houses and faces as stimuli, provided evidence for a dissociation of partial repetition effects in the parahippocampal place area and the fusiform face area, which can be explained by event file retrieval and downregulation of potentially conflicting stimulus information. In other fMRI studies, partial repetition effects have been observed in the parieto-occipital cortex in a visual search task (Pollmann, Weidner, Müller, Maertens, & von Cramon, 2006) and the fusiform cortex in a negative priming task (Dobbins, Schnyer, Verfaellie, & Schacter, 2004). In ERP studies that used the S1R1-S2R2 task, a partial repetition effect was found in the P300 component that was localized to the left parietal cortex (Friedrich et al., 2020; Kleimaker et al., 2020; Takacs, Zink, et al., 2020). Two other studies applied multivariate pattern analysis to temporal (Takacs, Mückschel, Roessner, & Beste, 2020) and time–frequency decomposed EEG data (Kikumoto & Mayr, 2020). Both studies provided evidence for event file retrieval and conjunctive representations of (rule-based) stimulus and response information. Takacs, Zink, et al. (2020) analyzed small-world network activity in EEG data and found evidence for partial repetition effects in theta (4–8 Hz) and alpha (8–12 Hz) oscillations.

With regard to DRBs, Opitz, Beste, and Stock (2020) examined ERPs in a DRB task in which both targets and distractors were mapped to responses. The results showed a partial repetition effect with regard to distractor prime–probe relation in the N450 component. Sources of the effect were localized to the right dorsolateral pFC and left inferior parietal cortex. Thus, together with the target–response binding studies above, the DRB study by Opitz et al. (2020) provides good evidence for partial repetition effects in brain activity that can be linked to the processing of event files and short-term stimulus–response bindings. Notably, however, all of this research examined brain activity that was time-locked to and started with probe encoding. Because multiple component processes contribute to the processing of event files during the encoding of the probe, including retrieval, conflict, unbinding, integration, and reconfiguration, it may be difficult to determine the exact functions of brain activities related to probe encoding. In contrast, in the RSI of the DRB task, a relatively "pure" measure in brain activity that is related to the integration and disintegration or decay of event files may be

empirically observable (see Hommel & Frings, 2020; Moeller et al., 2016; Frings, 2011).

This Study

The present study examined the EEG oscillatory correlates of short-term bindings in the DRB task with focus on the RSI, that is, the time interval between the prime response and the onset of the probe stimuli. Synchronizations of brain oscillations in different frequency bands have been suggested to constitute temporal short-term and long-term bindings that integrate distributed information in the brain with respect to perception, attention, and memory (Fell & Axmacher, 2011; Engel & Singer, 2001). Regarding motor activity and action control, in particular, alpha (8–14 Hz) and beta (15–25 Hz) oscillations have been shown to play an important role (Cheyne, 2013; Pastötter, Berchtold, & Bäuml, 2012). Alpha/beta power typically decreases (event-related desynchronization [ERD]; Pfurtscheller & Aranibar, 1977) during movement preparation and duration and strongly increases (event-related synchronization [ERS]; Pfurtscheller, 1992) shortly after movement execution. Whereas the ERD is predominant in alpha power, the postmovement ERS is predominant in beta power (Pfurtscheller & Lopes da Silva, 1999). Beta ERS (also called beta rebound) and alpha ERD have been source localized to the primary motor and sensorimotor cortices, located in the precentral and postcentral gyrus, respectively (Jurkiewicz, Gaetz, Bostan, & Cheyne, 2006). With respect to hand movements, beta ERS lasts for about 1–1.5 sec following movement execution and is more prominent contralateral to the side of the hand movement (McAllister et al., 2013; Jurkiewicz et al., 2006; Cassim et al., 2001). The exact functional role of postmovement beta ERS is not well understood. One interpretation is that beta ERS corresponds to cortical removal of excitation or idling (Pfurtscheller, Stancak, & Neuper, 1996). Alternatively, beta ERS has been suggested to reflect an active inhibition of the motor cortex by somatosensory feedback (Cassim et al., 2001). Engel and Fries (2010) proposed that beta synchronization signals the tendency of the motor system to maintain the status quo. In this sense, beta ERS might be related to temporal representations of individual actions, of the sort discussed in the action control literature. More specifically, therefore, this EEG study tested the new idea that postmovement beta ERS is related to short-term stimulus–response bindings.

This study took an individual differences approach, relating individual differences in behavior (i.e, individual DRB effects in RT and accuracy) to individual differences in neural oscillations (i.e., individual postmovement beta ERS effects). Neural variability both within and between individuals is considered a key dimension for understanding brain–behavior correlations (Waschke, Kloosterman, Obleser, & Garrett, 2021). Theoretically, individual (DRB and beta ERS) effects in within-subject designs are composed of mean group effects, meaningful individual deviations from the mean group effect, and measurement error (see Seghier & Price, 2018). Previous DRB research demonstrated significant correlations between individual DRB effects and other individual binding effects (e.g., response-effect binding; Moeller et al., 2016), which suggests that individual differences in the processing of stimulus–response bindings are (partially) meaningful and thus may be reliably related to other measures (e.g., postmovement beta ERS). In this study, behavioral DRB effects were related to individual ERS/ERD values following the prime response in the frequency range from 2 to 30 Hz. In different blocks, the RSI between the prime response and the onset of the probe display was either 500 or 2000 msec.

The following expectations were examined. First, on the group level, we expected to replicate the findings by Frings (2011) and Moeller et al. (2016) showing a larger DRB effect in RT in the RSI-500 condition than in the RSI-2000 condition. Also based on this earlier work, no difference in the DRB effect in accuracy between the two RSI conditions was expected. Second, on the individual level, according to the idea that postmovement beta ERS is linked to short-term stimulus–response bindings, positive correlations between the behavioral DRB scores and postmovement beta ERS in the RSI-500 interval and/or RSI-2000 interval were expected. Specifically, the finding of a positive correlation in the RSI-500 interval would provide evidence that postmovement beta ERS is related to individual differences in the just integrated stimulus–response bindings, whereas the finding of a positive correlation in the RSI-2000 interval would be more consistent with the view that postmovement beta ERS relates to individual differences in the disintegration or decay of event files over time. Third, beamformer and dynamic imaging of coherent sources (DICS) analyses were calculated to examine in an exploratory manner (i) the localization of possible hub regions of event file integration and disintegration or decay over time and (ii) the coherency of brain regions within sensorimotor networks of beta oscillations.

METHODS

Participants

Forty-five students (37 women, three left-handed, mean age = 25.0 years, *SD* = 4.2 years) from Trier University, Germany, participated in the study. G*Power (v3.1.9.4) sensitivity analysis for correlations indicated a required medium effect size of $|\rho| = .35$ (one-tailed) when alpha was set to .05 and power to .80 (Faul, Erdfelder, Buchner, & Lang, 2009). All participants reported normal or corrected-to-normal vision, gave written informed consent before examination, and received course credit or were paid 20 Euros for participation. No participant reported any history of neurological disease. The study

was conducted in accordance with the Declaration of Helsinki and was approved by the local ethical review committee at the University of Trier.

Stimuli

Participants performed a DRB task with prime–probe sequences, in which target letters were presented at central fixation and flanking distractor letters were presented left and right to the targets (Figure 1A). Target stimuli were the letters "D," "F," "J," and "K." The letters "D" and "F" were mapped to a response with the left index finger, whereas the letters "J" and "K" were mapped to a response with the right index finger. Different target letters were used in prime and probe displays of prime–probe sequences. Therefore, the combination of target letters was one-to-one in prime–probe sequences with RR ("D"→"F," "F"→"D," "J"→"K," "K"→"J") and was also controlled to be one-to-one in sequences with RC ("D"→"K," "K"→"D"; "F"→"J," "J"→"F"). Distractor stimuli were the letters "G," "H," "S," and "L." Distractors were always presented left and right to the target and not mapped to any responses. In prime–probe sequences with distractor repetition (DR), the same distractors were shown in prime and probe displays, whereas in sequences with distractor change (DC), different distractors were shown in prime and probe displays.

Experimental Design

In the prime–probe sequences, response relation between prime and probe (RR vs. RC) was varied orthogonally to distractor relation (DR vs. RC), resulting in four equally likely prime–probe combinations: RRDR, RRDC, RCDR, and RCDC. In addition to response relation and distractor relation, the prime–probe interval (RSI), that is, the interval between the prime response and the onset of the probe stimuli, was manipulated. In different blocks of the DRB experiment, the RSI was set to either 500 msec (RSI-500 condition) or 2000 msec (RSI-2000 condition).

Procedure

The experiment was conducted in a soundproof and electrically shielded EEG recording chamber. After preparation of electrodes, an eye tracker (Eyegaze System, LC Technologies), which was attached below the monitor, was calibrated for each individual participant. The calibration failed for eight participants; for those individuals, the eye-tracking control function (see below) was switched off. Before the DRB task, participants were instructed to place their left index finger on the key "C" and their right index finger on the key "M" of a standard German QWERTZ keyboard. Both keys were marked with red labels. Participants were asked to maintain fixation on the center of the screen during the DRB task. They should classify the target letters in both prime and probe displays. For the target letters "D" and "F," participants pressed the left key; for target letters "J" and "K," they pressed the right key. Target letters were shown in red font color in the middle of the screen. Participants were asked to respond as accurately and as quickly as possible. In addition, participants were instructed to ignore the distractors in both the prime and probe displays. Distractor letters were presented in green font color directly left and right of the targets. Target and distractor letters were approximately 1.2° in size. All stimuli were written in bold Courier New font. The screen background was black. Participants' viewing distance was 65 cm.

An experimental session consisted of 576 single trials, that is, prime–probe sequences, which were presented in six experimental blocks of 96 trials each. In three of these blocks, the RSI was set to 500 msec; in the other three blocks, the RSI was set to 2000 msec. The RSI-500 and RSI-2000 blocks alternated in order. Half of the participants started with an RSI-500 block, half with an RSI-2000 block.

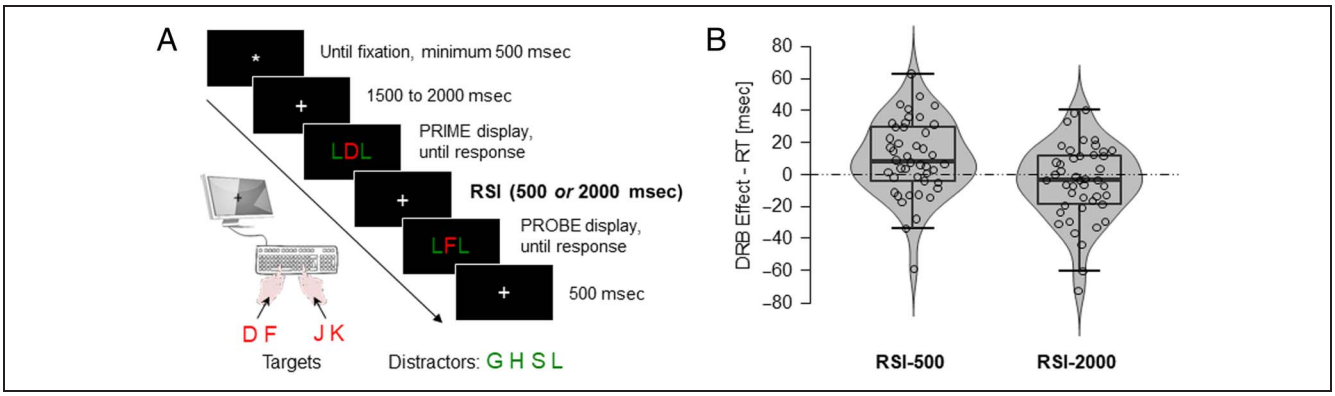

Figure 1. Experimental task and behavioral RT results. (A) Participants performed a sequential prime–probe DRB task, in which (red) target letters were presented at central fixation and (green) distractor letters were presented left and right to the targets. Prime–probe response relation (repetition vs change), distractor relation (repetition vs change), and length of the RSI (RSI-500 vs RSI-2000) were manipulated. (B) RT results indicated a significant DRB effect in the RSI-500 condition, but not in the RSI-2000 condition. Boxplots with violin and jitter elements of DRB-500 and DRB-2000 scores.

Between blocks, participants took a short break. Within each block, all predefined prime–probe target and distractor combinations were realized in a counterbalanced manner. Each single trial began with fixation of an asterisk, which was shown in the center of the screen for an interval of 500 msec (Figure 1A). If a participant did not fixate the asterisk at the end of this interval, the duration of the interval was prolonged until fixation.[1] Eye gaze was controlled by simultaneous eye tracking. Maximum permissible gaze deviation was set to 1.75° radius from the asterisk. After presentation of the asterisk, a fixation cross was shown with variable duration of 1500–2000 msec with a uniform probability distribution. Thereafter, the prime display was presented, showing the target letter (in red font) in the middle of the screen and the distractor letters (in green font) directly left and right of the target. Target and distractor letters remained on the screen until a response was made by the participant. No feedback was provided. After the response, the fixation cross was shown again. This time, the presentation time of the fixation cross was constant and depended on the RSI condition. In the RSI-500 condition, the fixation cross was presented for 500 msec, whereas in the RSI-2000 condition, it was presented for 2000 msec. Next, the probe display was shown, again showing the target letter (in red font) in the middle of the screen and the distractor letters (in green font) directly left and right of the target. The probe display remained on the screen until a response was made by the participant. Again no feedback was provided. Finally, a fixation cross of 500 msec duration was shown before the next single trial, that is, the next prime–probe sequence, started. To familiarize participants with the procedure, they were given one block of 32 practice trials (with 500 msec RSI) before the first experimental block started. Presentation of single trials and recording of behavioral responses was done with E-Prime software (v2.0, Psychology Software Tools). After the experiment, additional EEG and EOG data were collected for EOG calibration and correction.

Analysis of Behavioral Data

Both mean RT and error rate were analyzed. For each participant, trials with probe RT greater or equal to 900 msec were excluded from the RT analysis. In addition, only trials for which both prime and probe responses were correct were included in the RT analysis. Mean numbers of trials per participant included in the behavioral analysis of RT data were 261.0 (SD = 25.5) for the RSI-500 and 252.2 (SD = 25.4) for the RSI-2000 condition.

In the first step, behavioral data were analyzed with repeated-measures ANOVAs with the within-participants factors of Prime–Probe Response Relation (RR vs. RC), Prime–Probe Distractor Relation (DR vs. DC), and RSI (RSI-500 vs. RSI-2000). DRB is reflected in the interaction of the factors of response relation and distractor relation, because of faster and more accurate RRs (compared to RCs) if distractor stimuli are repeated than if distractor stimuli change, and faster and more accurate RCs (compared to RRs) if distractors change than if they are repeated. In the second step, individual DRB-500 and DRB-2000 scores were calculated by subtracting the individual distractor relation effect in RC trials (RCDC − RCDR) from the individual distractor relation effect in RR trials (RRDC − RRDR), separately for the two RSI conditions. These (double) difference scores reflect individual DRB effects, that is, the degree to which individuals integrate stimulus and response features. Note that both the DRB interaction effect on the group level and the DRB score on the individual level measure the integration of stimulus and response aspects but do not measure separate stimulus and response processing features. Planned comparisons of DRB-500 and DRB-2000 scores were calculated with paired-samples t tests. One-sample t tests were calculated to examine whether DRB-500 and DRB-2000 effects were different from 0.

Recording of EEG Data

Electrophysiological data were recorded from 65 Ag/AgCl electrodes, which were positioned according to the 10–10 electrode system with reference to FCz (EC80, Montage No. 1, Easycap). The ground was placed at location AFz. The EOG was recorded from four additional bipolar channels, positioned on the inferior and superior regions of the left eye and the outer canthi of both eyes, in order to monitor the vertical and horizontal EOG. Electrode-skin impedance was kept below 5 kΩ for all electrodes. Signals were digitalized with a sampling rate of 500 Hz and amplified between 0.016 and 250 Hz (BrainAmp, BrainVision Recorder, v1.20, Brain Products).

Preprocessing of EEG Data

EEG recordings were rereferenced off-line against average reference and EOG corrected by using calibration data and generating individual EOG artifact coefficients, as implemented in BESA Research (v7.0, BESA Software; see Ille, Berg, & Scherg, 2002). Remaining artifacts were marked by careful visual inspection. EEG signals of single channels showing heavy artifacts throughout a participant's session were interpolated using spline interpolation as implemented in BESA Research (mean number of channels per participant = 1.09; SD = 1.18; max = 4). EEG data were segmented into epochs ranging from −2 to 3 sec around the onset of prime responses. To avoid filter artifacts at the edges of the segments, further analyses were restricted to the interval of interest ranging from −1 to 2 sec around the onset of prime responses. Segments containing artifacts in the interval of interest and segments with prime or probe response errors were discarded from further analysis. Mean percentage of trials per participant included in the EEG data analysis were 85.5% (SD = 8.6%; min = 55.2%; max = 96.9%) for the RSI-500 and

84.6% (*SD* = 9.8%; min = 51.7%; max = 97.2%) for the RSI-2000 condition.

Analysis of EEG Data

Time–Frequency Transformation

The EEG data were transformed into the time–frequency domain using a complex demodulation algorithm, which is implemented in BESA Research (v7.0; see Hoechstetter et al., 2004). The algorithm consists of a multiplication of the time-domain signal with a complex periodic exponential function, having a frequency equal to the frequency under analysis, and subsequent low-pass filtering. The low-pass filter is a finite impulse response filter of Gaussian shape in the time-domain, which is related to the envelope of the moving window in wavelet analysis. The data were filtered in a frequency range from 2 to 30 Hz. Time resolution was set to 78.8 msec (full power width at half maximum, FWHM), and frequency resolution was set to 1.42 Hz (FWHM). Time–frequency data were exported in bins of 50 msec and 1 Hz. Event-related power changes, time-locked to the onset of the prime response, were determined by calculating the temporal–spectral evolution, that is, power changes for all time–frequency points with power increases or decreases at time point t and frequency f related to mean power at frequency f over a preceding baseline interval (Pfurtscheller & Aranibar, 1977). The baseline interval was set from −1000 to −750 msec before the onset of prime responses. Percent power increase indicates ERS, whereas percent power decrease indicates ERD (Pfurtscheller, 1992).

Cluster Analysis of Scalp EEG

ERS/ERD values in the time range from 0 to 2000 msec and the frequency range from 2 to 30 Hz, both in the RSI-500 and RSI-2000 conditions, were related to the individual DRB-500 and DRB-2000 scores using BESA Statistics (v2.0, BESA Software). That is, each DRB score was once correlated with the ERS/ERD values in the RSI condition (RSI-500 or RSI-2000) in which it was measured and once with the ERS/ERD values in the other RSI condition. For each of four correlation analyses (relating DRB-500 to ERS/ERD in the RSI-500 condition, DRB-500 to ERS/ERD in the RSI-2000 condition, DRB-2000 to ERS/ERD in the RSI-500 condition, and DRB-2000 to ERS/ERD in the RSI-2000 condition), a non-spatial-cluster-based permutation analysis was calculated first and a spatial analysis was calculated second.

In the non-spatial-cluster analysis, ERS/ERD values were averaged across the 65 electrodes and related to individual DRB scores by calculating Pearson's product–moment correlation. Two-tailed t tests were calculated for all ERS/ERD values (41 [50-msec time bins] × 29 [1-Hz frequency bins]). The sum of t values of adjacent time–frequency points that fell below a p value of .01 in the t test was calculated as a test statistic. Random permutation analysis was calculated based on 5000 randomization runs. In each randomization run, the (45) individual DRB scores were randomly assigned to the ERS/ERD data and t tests were calculated for each Pearson correlation at each time–frequency point. At the end of each run, t values of adjacent time–frequency points that fell below a p value of .01 were summed and the cluster with the highest sum of t values was kept. By these means, a null distribution of cluster sums was created from the 5000 random permutation runs, which was used to calculate the critical p value (p_{crit}) for an empirically derived time–frequency cluster (see Sassenhagen & Draschkow, 2019; Maris & Oostenveld, 2007).

Empirical clusters with a p_{crit} value below .05 went into spatial analysis. For each cluster, ERS/ERD values were averaged across data points of the cluster's maximum time range and maximum frequency range, separately for each electrode. These data were correlated with individual DRB scores. Two-tailed t tests were calculated for all electrodes. Spatial topographies of significant correlations were identified by considering those electrodes that fell below a p value of .01 in the t test. No additional cluster analysis was calculated. Thus, both clustered and scattered effects of conditions were considered in the spatial analysis. Note that the spatial analysis was calculated solely to describe the topography of correlation results because the results of the spatial analysis clearly depended on the results of the nonspatial analysis calculated in the step before (see Kriegeskorte, Simmons, Bellgowan, & Baker, 2009).

Beamformer Analysis

The Multiple Source Beamformer (MSBF), which is implemented in BESA Research (v7.0), was used to localize the neural sources of scalp-ERS/ERD in a predefined time–frequency range. The MSBF is a modified version of the linearly constrained minimum variance vector beamformer (Gross et al., 2001), which is based on the cross spectral density matrix to estimate oscillatory power of sources. For calculation of source-ERS/ERD values, the same 250-msec baseline interval as in the scalp EEG analysis was used. The time–frequency ranges were based on the results from the scalp-ERS/ERD cluster analysis. For each beamformer analysis, the frequency range was set to the scalp-ERS/ERD cluster's maximum frequency range. Because the MSBF needs the same duration of the baseline interval and the target interval for reliable source-ERS/ERD calculation, the time interval for beamformer analysis was set to be a multiple of 250 msec and the maximum time interval based on the scalp-ERS/ERD cluster's maximum time range was used. MSBF calculations for neighboring target intervals were averaged. MSBF results were superimposed onto a standard magnetic resonance (MR) image.

In the next step, brain–behavior correlations were calculated between the source-ERS/ERD values in the RSI-500 and RSI-2000 conditions and the behavioral DRB-500 and DRB-2000 effects. Cluster-based random permutation analyses and plotting of sources were done with BESA Statistics (v2.0). In each permutation analysis, paired t tests on the Pearson's product–moment correlations between source-ERS/ERD values and DRB scores were calculated for each voxel (voxel size was set to 7 mm in Talairach space). Clusters were identified by considering adjacent voxels that fell below a p value of .001 in the t test. The test statistic was the sum of t values of all voxels in a cluster. Five thousand random permutations were run to calculate the critical p value (p_{crit}) for an empirically derived time–frequency cluster. Anatomic labeling of neural sources was feasible using the MNI 2 Talairach Converter program (v1.3; Lacadie, Fulbright, Rajeevan, Constable, & Papademetris, 2008) and MRIcroGL (www.nitrc.org/projects/mricrogl/).

DICS

DICS was used for imaging cortico-cortical coherence in the brain. DICS as it is implemented in BESA Research (v7.0) closely follows Gross et al. (2001). DICS computation yields a 3-D image (on a standard MR template), with each voxel being assigned a coherence value to a predefined reference point (the seed). Coherence values are described as a neural activity index (in percent), which contrasts coherence in a target time–frequency bin with coherence of the same time–frequency bin in a baseline (same baseline as above). The reference point for each analysis was derived from the location of significant clusters in the MSBF correlation analysis. Settings of time–frequency ranges were the same as in the beamformer analysis. As in the MSBF analysis, calculations for neighboring target intervals were averaged and results were superimposed onto a standard MR image. Note that 3-D images indicate which brain areas showed the largest coherence with the seed; no contrasts or inferential statistics were calculated.

RESULTS

Behavioral Results

RT

Mean RTs are shown in Table 1. A three-way repeated-measures ANOVA with the factors of Response Relation (RR vs. RC), Distractor Relation (DR vs. DC), and RSI (RSI-500 vs. RSI-2000) showed significant main effects of Response Relation, $F(1, 44) = 20.76$, $MSE = 1250.71$, $p < .001$, $\eta_p^2 = .321$; Distractor Relation, $F(1, 44) = 4.35$, $MSE = 191.36$, $p = .043$, $\eta_p^2 = .090$; and RSI, $F(1, 44) = 72.95$, $MSE = 4570.72$, $p < .001$, $\eta_p^2 = .624$. These main effects were qualified by a significant two-way interaction between the factors of Response Relation and RSI, $F(1, 44) = 26.81$, $MSE = 406.61$, $p < .001$, $\eta_p^2 = .379$, and, more importantly, a significant three-way interaction between the three factors, $F(1, 44) = 8.64$, $MSE = 145.91$, $p = .005$, $\eta_p^2 = .164$. Planned comparison of DRB-500 and DRB-2000 indicated significantly larger DRB effects in the RSI-500 condition (mean RT = 9.91 msec; $SEM = 3.53$ msec; median RT = 7.67 msec) than in the RSI-2000 condition (mean RT = −5.06 msec; $SEM = 3.52$ msec; median RT = −.39 msec), $t(44) = 2.94$, $p = .005$, $d = .438$ (Figure 1B). Indeed, a reliable DRB effect was observed in the RSI-500 condition, $t(44) = 2.80$, $p = .007$, $d = .418$, but not in the RSI-2000 condition, $t(44) = -1.44$, $p = .16$.

Response Errors

Mean response errors are shown in Table 1. The three-way repeated-measures ANOVA with the factors of Response Relation (RR vs. RC), Distractor Relation (DR vs. DC), and RSI (RSI-500 vs. RSI-2000) indicated no significant main effects or interactions, all ps $> .05$. Therefore, brain–behavior correlations were calculated with individual DRB RT scores only.

EEG Results

Scalp EEG Results

Cluster-based permutation testing of significant correlations between ERS/ERD values (averaged over all scalp electrodes; see Figure 2A) and behavioral DRB-500 and DRB-2000 RT scores were calculated, separately for the RSI-500 and the RSI-2000 condition. The analyses showed no significant correlation cluster between ERS/ERD and DRB-500, neither in the RSI-500 condition, $p_{crit} = .54$, nor in the RSI-2000 condition, $p_{crit} = .16$ (Figure 2B). However, there were significant correlations between DRB-2000 and beta ERS in both the RSI-500 and the RSI-2000 conditions (Figure 2C). Indeed, DRB-2000 was positively related to beta ERS (approximately 17–24 Hz) in the RSI-2000 condition, in a cluster that extended approximately from 400 to 1300 msec after prime

Table 1. Behavioral Results

	RRDC_500	*RRDR_500*	*RCDC_500*	*RCDR_500*	*RRDC_2000*	*RRDR_2000*	*RCDC_2000*	*RCDR_2000*
RT	548.6 (11.8)	540.8 (12.3)	571.7 (12.1)	573.7 (12.2)	616.9 (9.4)	616.3 (9.6)	625.4 (9.3)	619.7 (9.1)
Errors	0.04 (0.01)	0.04 (0.01)	0.03 (0.01)	0.04 (0.01)	0.05 (0.01)	0.05 (0.01)	0.03 (0.00)	0.04 (0.01)

Means and *SEM*s.

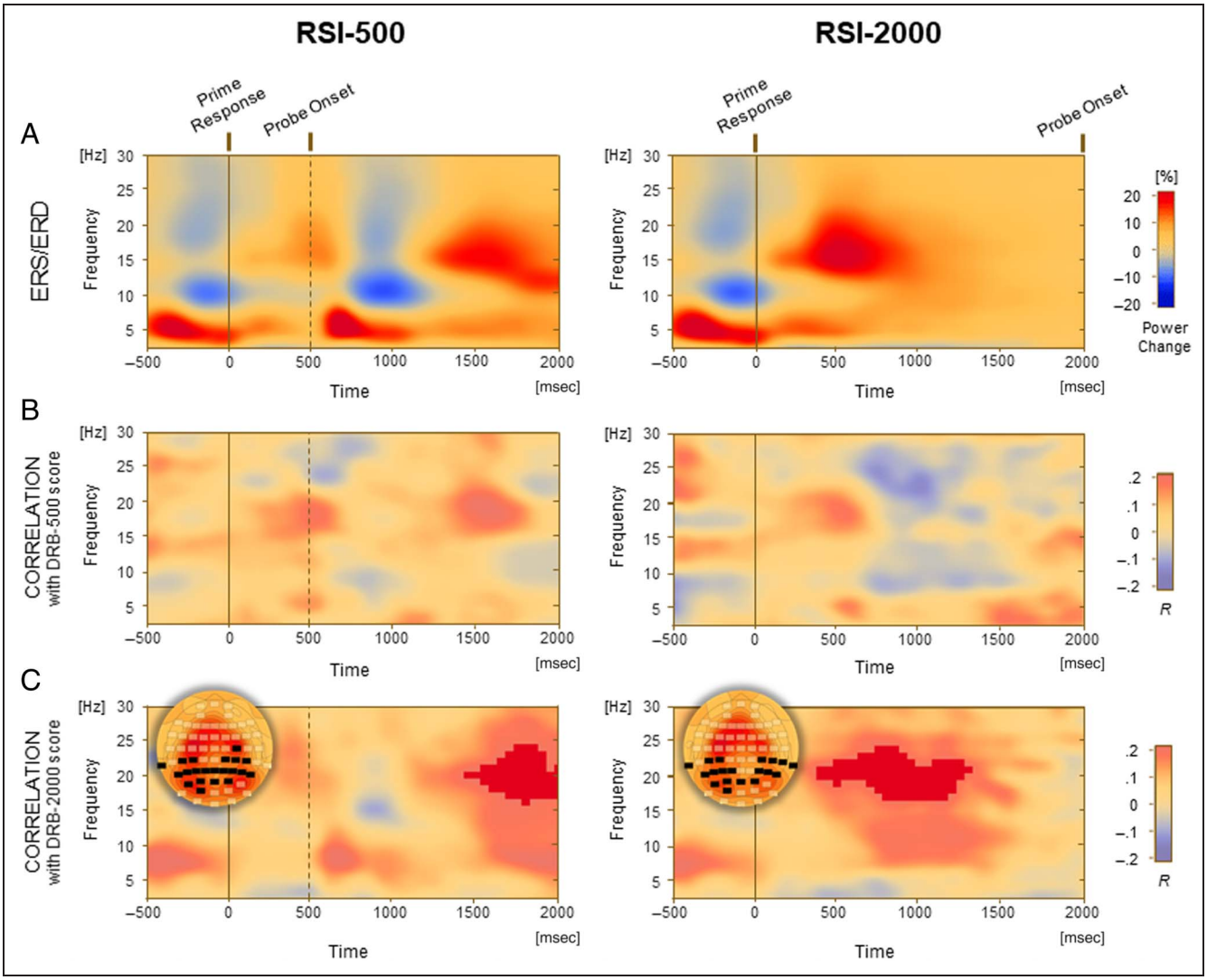

Figure 2. Scalp EEG results. (A) ERS/ERD values, stimulus-locked to the onset of prime responses and averaged over all scalp electrodes in the RSI-500 and the RSI-2000 condition. (B) No significant correlation cluster between ERS/ERD and DRB-500 was found, both in the RSI-500 and the RSI-2000 conditions. (C) Significant correlation clusters between beta ERS and DRB-2000 emerged both in the RSI-500 and the RSI-2000 conditions. Spatial analysis indicated tempo-parietal topographies of these effects. Electrodes showing significant correlations are depicted in black. Color coding of topographic maps denotes ERS/ERD from +40% to −40%.

responses, p_{crit} = .003.The same DRB effect (DRB-2000; measured in the RSI-2000 blocks) was also positively related to beta ERS (approximately 16–24 Hz) in the RSI-500 condition, in a cluster that extended approximately from 1450 to 2000 msec after prime responses, p_{crit} = .008. Note that this latter cluster was clearly later than probe onset and the probe response and can be interpreted as resulting from probe responding. Spatial analyses indicated that the DRB–2000 correlations to beta ERS were most pronounced over parietal electrode sites (see Figure 2C).

Beamformer Results

Neural sources of beta scalp-ERS/ERD in the respective time–frequency ranges, that is, from 1500 to 2000 msec after prime responses and from 16 to 24 Hz in the RSI-500 condition, and from 500 to 1250 msec after prime responses and from 17 to 24 Hz in the RSI-2000 condition, were localized to the motor cortex, with peak ERS in the left and right precentral gyrus (Brodmann's area [BA] 6; Figure 3A; note that the time intervals for the beamformer analysis were set to multiples of 250 msec, that is, the length of the baseline interval; see Methods section). Cluster analysis of brain–behavior correlations of source-ERS/ERD in the respective time–frequency ranges of the RSI-500 and RSI-2000 conditions to the behavioral DRB-500 and DRB-2000 RT scores revealed significant correlation clusters for DRB-2000 (Figure 3B), but zero correlation clusters for DRB-500. Indeed, in the RSI-2000 condition, DRB-2000 was positively related to a beta ERS cluster in the left middle occipital gyrus (Talairach coordinates $x = -38$, $y = -73$, $z = 24$; BA 19), p_{crit} =

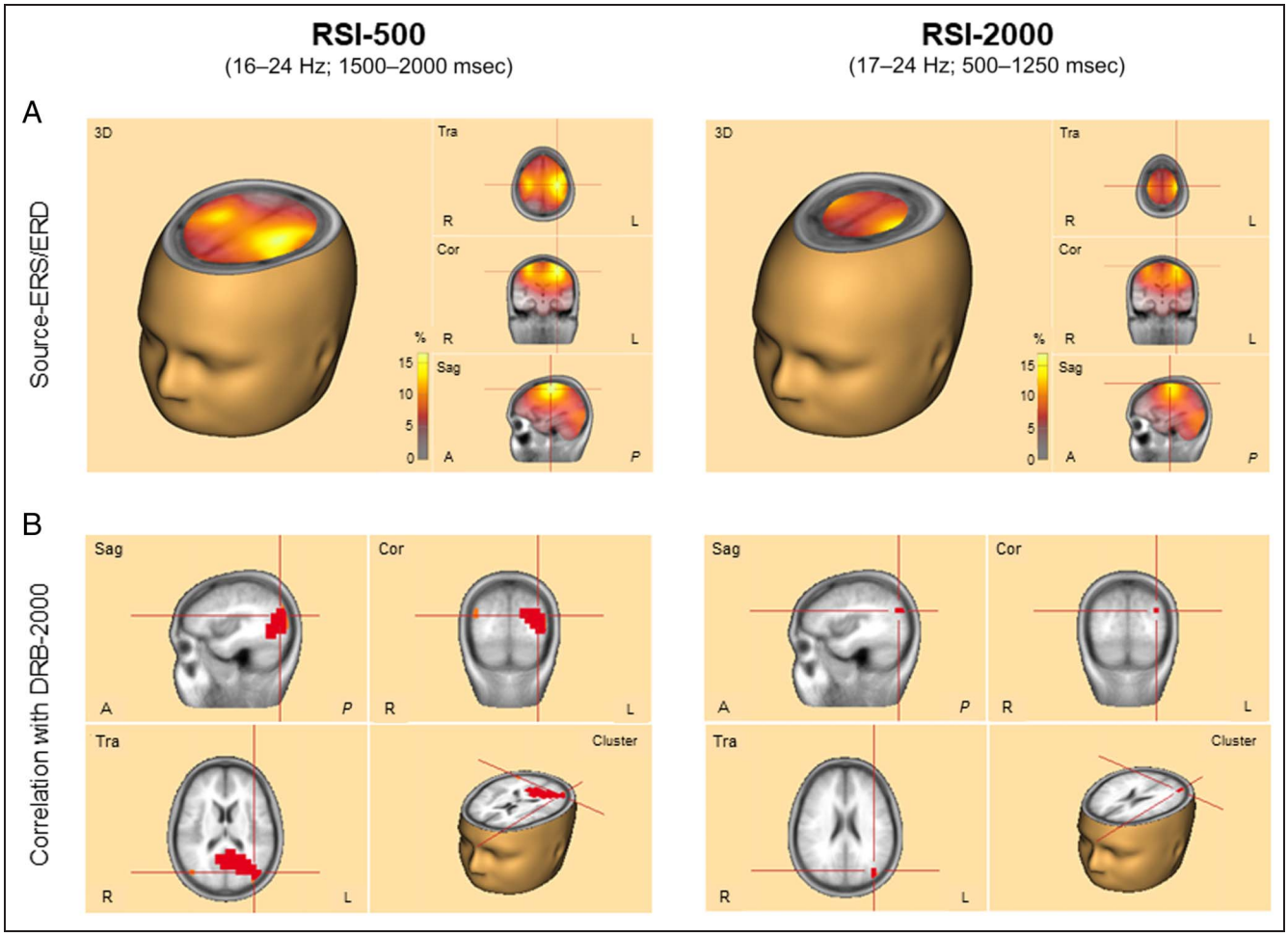

Figure 3. Beamformer results. (A) Neural sources of beta ERS were localized to the motor cortex, with peak beta ERS in the left and right precentral gyrus, both in the RSI-500 and RSI-2000 conditions. (B) Significant correlation clusters between beta ERS and DRB-2000 were observed in the left middle occipital gyrus in both the RSI-500 and RSI-2000 condition and the right middle occipital gyrus in the RSI-500 condition only. No significant correlation clusters between beta ERS and DRB-500 emerged.

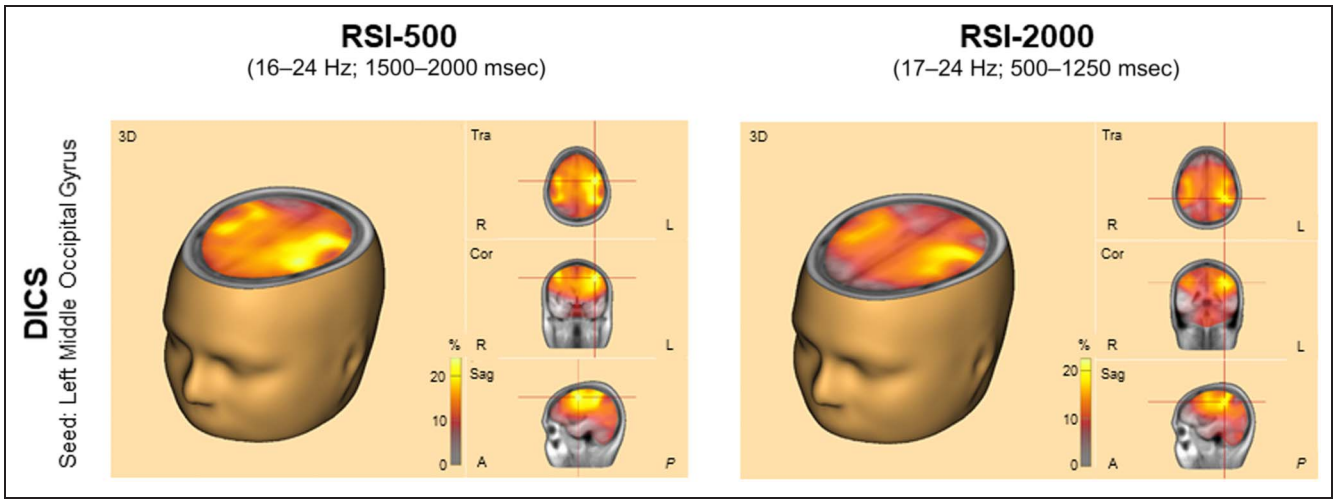

Figure 4. DICS results. Largest coherences with the seed in the left middle occipital gyrus were observed bilaterally in the motor cortex and the inferior parietal cortex, both in the RSI-500 and the RSI-2000 conditions.

.028. Consistently, in the RSI-500 condition, DRB-2000 was positively related to a beta ERS cluster in the left middle occipital gyrus (Talairach coordinates $x = -38$, $y = -73$, $z = 17$; BA 19), $p_{crit} = .003$, and, in addition, to a beta ERS cluster in the right middle occipital gyrus (Talairach coordinates: $x = 45$, $y = -73$, $z = 24$; BA 19), $p_{crit} = .024$.

DICS Results

DICS was used for imaging cortico-cortical coherence of beta oscillations between the left middle occipital gyrus (the seed), for which beta ERS clusters were consistently found to correlate with DRB-2000 in the RSI-500 and RSI-2000 conditions, and the single cortical voxels in source space. Settings of time–frequency ranges were the same as in the beamformer analysis above. The results of the DICS computation are shown in Figure 4. Both in the RSI-500 and the RSI-2000 conditions, the largest coherences with the seed in the left middle occipital gyrus were observed bilaterally in the motor cortex, with peak coherences in the left and right precentral gyrus (BA 6), and the left and right inferior parietal cortex, with peak coherences in the supramarginal gyrus (BA 40) and the angular gyrus (BA 39).

DISCUSSION

The behavioral results showed that the DRB effect in RT was significantly larger if the RSI was relatively short (500 msec) than when it was relatively long (2000 msec), which replicates the findings from previous work (Hommel & Frings, 2020; Moeller et al., 2016; Frings, 2011). In fact, the behavioral DRB effect in RT was significant in the RSI-500 but not in the RSI-2000 condition (see also Frings, 2011). Thus, the behavioral RT results replicated the findings from earlier DRB work. The scalp EEG results revealed a significant correlation of individual differences in DRB-2000 (i.e., DRB scores in the RSI-2000 condition) with beta ERS (approximately 16–24 Hz) in both the RSI-500 and the RSI-2000 condition over parietal sites. Notably, the correlation followed in time the prime response in the RSI-2000 condition and the probe response in the RSI-500 condition. That is, participants who reached larger DRB scores in the RSI-2000 condition also showed larger beta ERS after responses that were followed by an undisturbed time window of at least 2000 msec. Beamformer analysis localized the postmovement beta ERS in the precentral gyrus, which is consistent with earlier work (Jurkiewicz et al., 2006). More importantly, the correlation between DRB-2000 scores and postmovement beta ERS was localized to the left (and in the RSI-500 condition also to the right) middle occipital gyrus (BA 19), suggesting that the middle occipital gyrus is a hub region for short-term stimulus–response bindings. DICS analysis revealed that the left middle occipital gyrus is further synchronized in the beta frequency range to the precentral gyrus (BA 6) and the parietal cortex (BA 39/40), indicating a sensorimotor network of beta oscillations that relates to visual DRB via the occipital hub.

Note that, at the group level, a significant DRB effect in RT was observed in the RSI-500 condition but not in the RSI-2000 condition, which replicates the finding by Frings (2011). Yet, at the individual-differences level, beta ERS was significantly correlated with the behavioral DRB-2000 score but not with the DRB-500 score. The significant correlation between beta ERS and DRB-2000 suggests that postmovement beta ERS (in the RSI-2000 condition after the prime response, but also in the RSI-500 condition after the probe response) is linked to individual differences in the disintegration or decay of event files. At least two possibilities arise regarding the nonfinding of a significant correlation between beta ERS and DRB-500. First, the integration strength of event files may in fact be unrelated to beta ERS and thus have a different neural signature. Second, the integration strength may be in fact related to beta ERS; however, differences in individual beta ERS that are due to individual differences in the integration process are less reliably observed than individual differences in beta ERS that are related to disintegration and decay.

With regard to the sensorimotor function of beta oscillations, postmovement beta ERS has been linked to cortical removal of excitation or idling (Pfurtscheller et al., 1996), active inhibition of the motor cortex by somatosensory feedback (Cassim et al., 2001), and the tendency of the motor system to maintain a status quo (Engel & Fries, 2010). Possibly specifying the latter suggestion, this study indicates that postmovement beta ERS is related to short-term stimulus–response bindings. Specifically, the results suggest that postmovement ERS is related to individual differences in the short-term storage and decay or disintegration of DRBs. This view is supported by the finding that the correlation between beta ERS and DRB-2000 was positive in direction. In fact, if beta ERS reflected inhibition or a resetting process, a negative correlation between beta ERS and DRB-2000 should have been observed. Regarding the time course of beta ERS, we found the synchronization to last for about 1–1.5 sec following movement execution, which replicates the findings from earlier work (McAllister et al., 2013; Jurkiewicz et al., 2006; Cassim et al., 2001). Interestingly, this time course of beta ERS nicely fits with the time course of behavioral DRB effects in RT, which have been observed to be clearly present if the probe is presented 500 msec after the prime response but reduced or even absent if the probe is presented 2000 msec after the prime response (Hommel & Frings, 2020; Moeller et al., 2016; Frings, 2011). Thus, the observed time range of postmovement beta ERS may reflect the exact time window during which short-term DRBs integrate, are stored within a short time period, and disintegrate. Indeed, the idea that beta ERS is related to such short-term memory function is in line with previous studies that linked beta synchronization to short-term

attention and working memory (Pastötter, Dreisbach, & Bäuml, 2013; Siegel, Warden, & Miller, 2009; Deiber et al., 2007; Gross et al., 2004).

Exploratory beamformer and DICS analyses revealed a sensorimotor network of beta oscillations that was linked to behavioral DRB-2000 via the left middle occipital gyrus as a hub. Needless to say that EEG has an excellent temporal resolution but, in comparison to other imaging methods like functional magnetic resonance imaging, a relatively low spatial resolution. Moreover, beamformer and DICS techniques rely on inverse modeling of EEG data, and therefore estimated sources in the brain should be interpreted with caution. Having said this, we think that the beamformer and DICS analyses revealed some very interesting and meaningful results. In the neuroscientific literature, it is a prominent idea that different ventral and dorsal visual systems in the human brain provide different information for perception and action (Goodale & Milner, 1992; Mishkin, Ungerleider, & Macko, 1983). The middle occipital gyrus (BA 19) is considered to be part of the dorsal visual system; it receives inputs from the primary and secondary visual cortex and projects to the posterior parietal cortex. The dorsal visual system can be divided into a dorso-dorsal and a ventro-dorsal stream (Binkofski & Buxbaum, 2013; Rizzolatti & Matelli, 2003), with the latter being crucially involved in the interaction of perception and action. Interestingly now, the present DICS results provided evidence for a network of beta oscillations exactly along the ventro-dorsal stream, which passes from visual cortex to the angular gyrus (BA 39), the supramarginal gyrus (BA 40), and the lateral precentral gyrus (BA 6). Thus, the present results propose the new idea that short-term stimulus–response bindings, at least in the present visual DRB task, are partially processed along the vento-dorsal stream. Future imaging studies with high spatial resolution should investigate this new idea in more detail.

In this study, we analyzed bindings between distractor stimuli and responses and found that this binding effect correlates with beta ERS approximately from 400 to 1300 msec after integration. Notably, this is also the time frame within which complete decay of DRB takes place: Whereas DRB-effects are reliably measurable at 500 msec after integration, the same effect is typically not found at 2000 msec after integration (e.g., Frings, 2011; see also the present behavioral results). Bindings between target–stimuli (e.g., Hommel & Frings, 2020; Hommel & Colzato, 2004) or effect-stimuli (e.g., Herwig & Waszak, 2012) and responses last for longer periods of time. Target–response bindings are still measurable after 4 sec following integration (Hommel & Colzato, 2004) and have been shown to completely decay within 5–6 sec (Hommel & Frings, 2020). Response–effect bindings (Herwig & Waszak, 2012) and also bindings between individually planned and executed responses (Moeller & Frings, 2019) were even reported after a delay of 6 sec. If the decay function of bindings is generally related with beta ERS, we would expect a similar correlation between binding effects and beta ERS as found in this study either for longer or for later time windows regarding target or effect stimuli. Thereby, although the left middle occipital gyrus was found to be a possible hub region for short-term stimulus–response bindings in the present visual DRB task, different hubs may be expected for different feature modalities (e.g., auditory, haptic) of stimuli and for bindings between responses. Examining these issues is a high priority for future research.

Although this study was on the short-term aftereffects of a single encounter of a stimulus together with a response, another important focus in action control research is on long-term learning of repeated pairings of stimuli and responses. Both the study of short-term bindings and the study of long-term learning are essential to get a better understanding of how humans interact with their environment in an adaptive way (Colzato, Raffone, & Hommel, 2006). Moeller and Frings (2017) provided behavioral evidence that short-term bindings and long-term contingency learning of stimulus–response associations are dissociable. Replicating the findings of Frings (2011) and consistent with the present results, Moeller and Frings (2017) showed a significant DRB effect in RT in the RSI-500 condition but not in the RSI-2000 condition, indicating that short-term DRBs disintegrate within a short period of time. In contrast, long-term contingency learning effects were found to be significant for slow-paced learning in the RSI-2000 but not for fast-paced learning in the RSI-500 condition, indicating that contingency learning needs sufficient time. On the other hand, in every situation that creates long-term learning of stimulus–response associations, short-term bindings should be involved. Therefore, partly overlapping brain activations of short-term bindings and encoding events that lead to long-term learning should be observed. Indeed, an fMRI study by Dobbins et al. (2004) demonstrated that the left fusiform cortex and its surrounding areas (BA 19/37) show a partial repetition effect in long-term learning of stimulus–response associations in the repetition priming task. This topography of this effect is largely consistent with the present beamformer localization of the EEG-DRB correlation effect (BA 19). Future EEG and fMRI studies are needed to examine the interplay of mechanisms relating to short-term bindings and long-term learning of stimulus–response associations within single experiments in more detail. In addition, future EEG work may like to examine the roles of stimulus–response and response–response bindings (see Moeller & Frings, 2019) for motor sequence learning (see Abrahamse, Jiménez, Verwey, & Clegg, 2010, for a review), which has also been linked to beta oscillatory activity and premovement beta ERD in particular (Pollok, Latz, Krause, Butz, & Schnitzler, 2014).

Conclusions

To conclude, short-term binding and retrieval of stimulus–response information are considered as different and

separable processes that independently contribute to sequential prime–probe binding effects in the S1R1-S2R2 and DRB task (Frings et al., 2020). Previous fMRI and EEG work focused on partial repetition effects in response to the encoding of probe information, to which, arguably, multiple component processes may contribute. In contrast, this EEG study provided a relatively "pure" brain oscillatory measure of short-term stimulus–response binding between the encoding of prime and probe information. It demonstrates that postmovement beta ERS is related to the (dis)integration of event files and suggests that the left middle occipital gyrus is a hub region for the short-term storage of (visual) distractor–response information.

Acknowledgments

The authors thank T. Brinkmann, L. Grunitz, K. Noll, and J. Paulus for their help with data collection and experimental setup.

Reprint requests should be sent to Bernhard Pastötter, Department of Psychology; University of Trier, 54296 Trier, Germany, or via e-mail: pastoetter@uni-trier.de.

Author Contributions

Bernhard Pastötter: Conceptualization; EEG analysis; Writing—Original draft. Birte Moeller: Conceptualization; Behavioral analysis; Writing—Review & editing. Christian Frings: Conceptualization; Writing—Review & editing.

Diversity in Citation Practices

A retrospective analysis of the citations in every article published in this journal from 2010 to 2020 has revealed a persistent pattern of gender imbalance: Although the proportions of authorship teams (categorized by estimated gender identification of first author/last author) publishing in the *Journal of Cognitive Neuroscience (JoCN)* during this period were M(an)/M = .408, W(oman)/M = .335, M/W = .108, and W/W = .149, the comparable proportions for the articles that these authorship teams cited were M/M = .579, W/M = .243, M/W = .102, and W/W = .076 (Fulvio et al., *JoCN*, 33:1, pp. 3–7). Consequently, *JoCN* encourages all authors to consider gender balance explicitly when selecting which articles to cite and gives them the opportunity to report their article's gender citation balance. The authors of this article report its proportions of citations by gender category to be as follows: M/M = .727, W/M = .164, M/W = .073, and W/W = .036.

Data Availability

Behavioral data (both raw and aggregated), analysis scripts for behavioral raw data, and aggregated EEG data are provided on the Open Science Framework at https://osf.io/br67v/ [DOI 10.17605/OSF.IO/BR67V]. The raw EEG data are not included because of space constraints, but are available from the first author on request.

Note

1. For those eight participants for whom the eye tracker calibration failed, the asterisk was shown for a fixed time interval of 500 msec in all single trials.

REFERENCES

Abrahamse, E. L., Jiménez, L., Verwey, W. B., & Clegg, B. A. (2010). Representing serial action and perception. *Psychonomic Bulletin & Review*, *17*, 603–623. **DOI:** https://doi.org/10.3758/PBR.17.5.603, **PMID:** 21037157

Binkofski, F., & Buxbaum, L. J. (2013). Two action systems in the human brain. *Brain and Language*, *127*, 222–229. **DOI:** https://doi.org/10.1016/j.bandl.2012.07.007, **PMID:** 22889467, **PMCID:** PMC4311762

Cassim, F., Monaca, C., Szurhaj, W., Bourriez, J. L., Defebvre, L., Derambure, P., et al. (2001). Does post-movement beta synchronization reflect an idling motor cortex? *NeuroReport*, *12*, 3859–3863. **DOI:** https://doi.org/10.1097/00001756-200112040-00051, **PMID:** 11726809

Cheyne, D. O. (2013). MEG studies of sensorimotor rhythms: A review. *Experimental Neurology*, *245*, 27–39. **DOI:** https://doi.org/10.1016/j.expneurol.2012.08.030, **PMID:** 22981841

Colzato, L. S., Raffone, A., & Hommel, B. (2006). What do we learn from binding features? Evidence for multilevel feature integration. *Journal of Experimental Psychology: Human Perception and Performance*, *32*, 705–716. **DOI:** https://doi.org/10.1037/0096-1523.32.3.705, **PMID:** 16822133

Deiber, M.-P., Missonnier, P., Bertrand, O., Gold, G., Fazio-Costa, L., Ibanez, V., et al. (2007). Distinction between perceptual and attentional processing in working memory tasks: A study of phase-locked and induced oscillatory brain dynamics. *Journal of Cognitive Neuroscience*, *19*, 158–172. **DOI:** https://doi.org/10.1162/jocn.2007.19.1.158, **PMID:** 17214572

Dobbins, I. G., Schnyer, D. M., Verfaellie, M., & Schacter, D. L. (2004). Cortical activity reductions during repetition priming can result from rapid response learning. *Nature*, *428*, 316–319. **DOI:** https://doi.org/10.1038/nature02400, **PMID:** 14990968

Engel, A. K., & Fries, P. (2010). Beta-band oscillations—Signalling the status quo? *Current Opinion in Neurobiology*, *20*, 156–165. **DOI:** https://doi.org/10.1016/j.conb.2010.02.015, **PMID:** 20359884

Engel, A. K., & Singer, W. (2001). Temporal binding and the neural correlates of sensory awareness. *Trends in Cognitive Sciences*, *5*, 16–25. **DOI:** https://doi.org/10.1016/S1364-6613(00)01568-0, **PMID:** 11164732

Faul, F., Erdfelder, E., Buchner, A., & Lang, A. G. (2009). Statistical power analyses using G* Power 3.1: Tests for correlation and regression analyses. *Behavior Research Methods*, *41*, 1149–1160. **DOI:** https://doi.org/10.3758/BRM.41.4.1149, **PMID:** 19897823

Fell, J., & Axmacher, N. (2011). The role of phase synchronization in memory processes. *Nature Reviews Neuroscience*, *12*, 105–118. **DOI:** https://doi.org/10.1038/nrn2979, **PMID:** 21248789

Fournier, L. R., Behmer, L. P., & Stubblefield, A. M. (2014). Interference due to shared features between action plans is influenced by working memory span. *Psychonomic Bulletin & Review*, *21*, 1524–1529. **DOI:** https://doi.org/10.3758/s13423-014-0627-0, **PMID:** 24715506

Friedrich, J., Verrel, J., Kleimaker, M., Münchau, A., Beste, C., & Bäumer, T. (2020). Neurophysiological correlates of

perception–action binding in the somatosensory system. *Scientific Reports*, *10*, 1–12. **DOI:** https://doi.org/10.1038/s41598-020-71779-0, **PMID:** 32908197, **PMCID:** PMC7481208

Fries, P., Fernandez, G., & Jensen, O. (2003). When neurons form memories. *Trends in Neurosciences*, *26*, 123–124. **DOI:** https://doi.org/10.1016/S0166-2236(03)00023-7, **PMID:** 12591213

Frings, C. (2011). On the decay of distractor–response episodes. *Experimental Psychology*, *58*, 125–131. **DOI:** https://doi.org/10.1027/1618-3169/a000077, **PMID:** 20705549

Frings, C., Hommel, B., Koch, I., Rothermund, K., Dignath, D., Giesen, C., et al. (2020). Binding and retrieval in action control (BRAC). *Trends in Cognitive Sciences*, *24*, 375–387. **DOI:** https://doi.org/10.1016/j.tics.2020.02.004, **PMID:** 32298623

Frings, C., & Rothermund, K. (2011). To be or not to be... included in an event file: Integration and retrieval of distractors in stimulus–response episodes is influenced by perceptual grouping. *Journal of Experimental Psychology: Learning, Memory, and Cognition*, *37*, 1209–1227. **DOI:** https://doi.org/10.1037/a0023915, **PMID:** 21707218

Frings, C., Rothermund, K., & Wentura, D. (2007). Distractor repetitions retrieve previous responses to targets. *Quarterly Journal of Experimental Psychology*, *60*, 1367–1377. **DOI:** https://doi.org/10.1080/17470210600955645, **PMID:** 17853245

Goodale, M. A., & Milner, A. D. (1992). Separate visual pathways for perception and action. *Trends in Neurosciences*, *15*, 20–25. **DOI:** https://doi.org/10.1016/0166-2236(92)90344-8, **PMID:** 1374953

Gross, J., Kujala, J., Hämäläinen, M., Timmermann, L., Schnitzler, A., & Salmelin, R. (2001). Dynamic imaging of coherent sources: Studying neural interactions in the human brain. *Proceedings of the National Academy of Sciences, U.S.A.*, *98*, 694–699. **DOI:** https://doi.org/10.1073/pnas.98.2.694, **PMID:** 11209067, **PMCID:** PMC14650

Gross, J., Schmitz, F., Schnitzler, I., Kessler, K., Shapiro, K., Hommel, B., et al. (2004). Modulation of long-range neural synchrony reflects temporal limitations of visual attention in humans. *Proceedings of the National Academy of Sciences, U.S.A.*, *101*, 13050–13055. **DOI:** https://doi.org/10.1073/pnas.0404944101, **PMID:** 15328408, **PMCID:** PMC516515

Henson, R., Eckstein, D., Waszak, F., Frings, C., & Horner, A. (2014). Stimulus–response bindings in priming. *Trends in Cognitive Sciences*, *18*, 376–384. **DOI:** https://doi.org/10.1016/j.tics.2014.03.004, **PMID:** 24768034, **PMCID:** PMC4074350

Herwig, A., & Waszak, F. (2012). Action-effect bindings and ideomotor learning in intention- and stimulus-based actions. *Frontiers in Psychology*, *3*, 444. **DOI:** https://doi.org/10.3389/fpsyg.2012.00444, **PMID:** 23112785, **PMCID:** PMC3481004

Hoechstetter, K., Bornfleth, H., Weckesser, D., Ille, N., Berg, P., & Scherg, M. (2004). BESA source coherence: A new method to study cortical oscillatory coupling. *Brain Topography*, *16*, 233–238. **DOI:** https://doi.org/10.1023/B:BRAT.0000032857.55223.5d, **PMID:** 15379219

Hommel, B. (1998). Event files: Evidence for automatic integration of stimulus–response episodes. *Visual Cognition*, *5*, 183–216. **DOI:** https://doi.org/10.1080/713756773

Hommel, B. (2004). Event files: Feature binding in and across perception and action. *Trends in Cognitive Sciences*, *8*, 494–500. **DOI:** https://doi.org/10.1016/j.tics.2004.08.007, **PMID:** 15491903

Hommel, B., & Colzato, L. (2004). Visual attention and the temporal dynamics of feature integration. *Visual Cognition*, *11*, 483–521. **DOI:** https://doi.org/10.1080/13506280344000400

Hommel, B., & Frings, C. (2020). The disintegration of event files over time: Decay or interference? *Psychonomic Bulletin & Review*, *27*, 751–757. **DOI:** https://doi.org/10.3758/s13423-020-01738-3, **PMID:** 32378119, **PMCID:** PMC7399672

Hommel, B., Müsseler, J., Aschersleben, G., & Prinz, W. (2001). The theory of event coding (TEC): A framework for perception and action planning. *Behavioral and Brain Sciences*, *24*, 849–878. **DOI:** https://doi.org/10.1017/s0140525x01000103, **PMID:** 12239891

Ille, N., Berg, P., & Scherg, M. (2002). Artifact correction of the ongoing EEG using spatial filters based on artifact and brain signal topographies. *Journal of Clinical Neurophysiology*, *19*, 113–124. **DOI:** https://doi.org/10.1016/0013-4694(92)90133-3, **PMID:** 1376667

Jurkiewicz, M. T., Gaetz, W. C., Bostan, A. C., & Cheyne, D. (2006). Post-movement beta rebound is generated in motor cortex: Evidence from neuromagnetic recordings. *Neuroimage*, *32*, 1281–1289. **DOI:** https://doi.org/10.1016/j.neuroimage.2006.06.005, **PMID:** 16863693

Kahneman, D., Treisman, A., & Gibbs, B. J. (1992). The reviewing of object files: Object-specific integration of information. *Cognitive Psychology*, *24*, 175–219. **DOI:** https://doi.org/10.1016/0010-0285(92)90007-O

Kikumoto, A., & Mayr, U. (2020). Conjunctive representations that integrate stimuli, responses, and rules are critical for action selection. *Proceedings of the National Academy of Sciences, U.S.A.*, *117*, 10603–10608. **DOI:** https://doi.org/10.1073/pnas.1922166117, **PMID:** 32341161, **PMCID:** PMC7229692

Kleimaker, M., Takacs, A., Conte, G., Onken, R., Verrel, J., Bäumer, T., et al. (2020). Increased perception-action binding in Tourette syndrome. *Brain*, *143*, 1934–1945. **DOI:** https://doi.org/10.1093/brain/awaa111, **PMID:** 32464659

Kriegeskorte, N., Simmons, W. K., Bellgowan, P. S., & Baker, C. I. (2009). Circular analysis in systems neuroscience: The dangers of double dipping. *Nature Neuroscience*, *12*, 535–540. **DOI:** https://doi.org/10.1016/0013-4694(92)90133-3, **PMID:** 1376667

Kühn, S., Keizer, A. W., Colzato, L. S., Rombouts, S. A., & Hommel, B. (2011). The neural underpinnings of event-file management: Evidence for stimulus-induced activation of and competition among stimulus–response bindings. *Journal of Cognitive Neuroscience*, *23*, 896–904. **DOI:** https://doi.org/10.1162/jocn.2010.21485, **PMID:** 20377359

Lacadie, C. M., Fulbright, R. K., Rajeevan, N., Constable, R. T., & Papademetris, X. (2008). More accurate Talairach coordinates for neuroimaging using non-linear registration. *Neuroimage*, *42*, 717–725. **DOI:** https://doi.org/10.1016/j.neuroimage.2008.04.240, **PMID:** 18572418, **PMCID:** PMC2603575

Maris, E., & Oostenveld, R. (2007). Nonparametric statistical testing of EEG- and MEG-data. *Journal of Neuroscience Methods*, *164*, 177–190. **DOI:** https://doi.org/10.1016/j.jneumeth.2007.03.024, **PMID:** 17517438

McAllister, C. J., Rönnqvist, K. C., Stanford, I. M., Woodhall, G. L., Furlong, P. L., & Hall, S. D. (2013). Oscillatory beta activity mediates neuroplastic effects of motor cortex stimulation in humans. *Journal of Neuroscience*, *33*, 7919–7927. **DOI:** https://doi.org/10.1016/j.expneurol.2012.08.030, **PMID:** 22981841

Mishkin, M., Ungerleider, L. G., & Macko, K. A. (1983). Object vision and spatial vision: Two cortical pathways. *Trends in Neurosciences*, *6*, 414–417. **DOI:** https://doi.org/10.1016/0166-2236(83)90190-X

Moeller, B., & Frings, C. (2017). Dissociation of binding and learning processes. *Attention, Perception, & Psychophysics*, *79*, 2590–2605. **DOI:** https://doi.org/10.3758/s13414-017-1393-7, **PMID:** 28752283

Moeller, B., & Frings, C. (2019). From simple to complex actions: Response–response bindings as a new approach to action sequences. *Journal of Experimental Psychology: General*, *148*, 174–183. **DOI:** https://doi.org/10.1037/xge0000483, **PMID:** 30211579

Moeller, B., Pfister, R., Kunde, W., & Frings, C. (2016). A common mechanism behind distractor–response and response–effect binding? *Attention, Perception, & Psychophysics*, *78*, 1074–1086. **DOI:** https://doi.org/10.3758/s13414-016-1063-1, **PMID:** 26810573

Opitz, B. (2010). Neural binding mechanisms in learning and memory. *Neuroscience & Biobehavioral Reviews*, *34*, 1036–1046. **DOI:** https://doi.org/10.1016/j.neubiorev.2009.11.001, **PMID:** 19914286

Opitz, A., Beste, C., & Stock, A. K. (2020). Using temporal EEG signal decomposition to identify specific neurophysiological correlates of distractor–response bindings proposed by the theory of event coding. *Neuroimage*, *209*, 116524. **DOI:** https://doi.org/10.1016/j.neuroimage.2020.116524, **PMID:** 31926281

Packard, M. G., & Knowlton, B. J. (2002). Learning and memory functions of the basal ganglia. *Annual Review of Neuroscience*, *25*, 563–593. **DOI:** https://doi.org/10.1146/annurev.neuro.25.112701.142937, **PMID:** 26810573

Pastötter, B., Berchtold, F., & Bäuml, K.-H. T. (2012). Oscillatory correlates of controlled speed-accuracy tradeoff in a response-conflict task. *Human Brain Mapping*, *33*, 1834–1849. **DOI:** https://doi.org/10.1002/hbm.21322, **PMID:** 21618665, **PMCID:** PMC6869900

Pastötter, B., Dreisbach, G., & Bäuml, K.-H. T. (2013). Dynamic adjustments of cognitive control: Oscillatory correlates of the conflict adaptation effect. *Journal of Cognitive Neuroscience*, *25*, 2167–2178. **DOI:** https://doi.org/10.1162/jocn_a_00474, **PMID:** 24001006

Patterson, K., Nestor, P. J., & Rogers, T. T. (2007). Where do you know what you know? The representation of semantic knowledge in the human brain. *Nature Reviews Neuroscience*, *8*, 976–987. **DOI:** https://doi.org/10.1038/nrn2277, **PMID:** 18026167

Pfurtscheller, G. (1992). Event-related synchronization (ERS): An electrophysiological correlate of cortical areas at rest. *Electroencephalography and Clinical Neurophysiology*, *83*, 62–69. **DOI:** https://doi.org/10.1016/0013-4694(92)90133-3, **PMID:** 1376667

Pfurtscheller, G., & Aranibar, A. (1977). Event-related cortical desynchronization detected by power measurements of scalp EEG. *Electroencephalography and Clinical Neurophysiology*, *42*, 817–826. **DOI:** https://doi.org/10.1016/0013-4694(77)90235-8, **PMID:** 67933

Pfurtscheller, G., & Lopes da Silva, F. H. (1999). Event-related EEG/MEG synchronization and desynchronization: Basic principles. *Clinical Neurophysiology*, *110*, 1842–1857. **DOI:** https://doi.org/10.1016/S1388-2457(99)00141-8, **PMID:** 10576479

Pfurtscheller, G., Stancak, A., & Neuper, C. (1996). Post-movement beta synchronization. A correlate of an idling motor area? *Electroencephalography and Clinical Neurophysiology*, *98*, 281–293. **DOI:** https://doi.org/10.1016/0013-4694(95)00258-8, **PMID:** 8641150

Pollmann, S., Weidner, R., Müller, H. J., Maertens, M., & von Cramon, D. Y. (2006). Selective and interactive neural correlates of visual dimension changes and response changes. *Neuroimage*, *30*, 254–265. **DOI:** https://doi.org/10.1016/j.neuroimage.2005.09.013, **PMID:** 16263311

Pollok, B., Latz, D., Krause, V., Butz, M., & Schnitzler, A. (2014). Changes of motor-cortical oscillations associated with motor learning. *Neuroscience*, *275*, 47–53. **DOI:** https://doi.org/10.1016/j.neuroscience.2014.06.008, **PMID:** 24931763

Rizzolatti, G., & Matelli, M. (2003). Two different streams form the dorsal visual system: Anatomy and functions. *Experimental Brain Research*, *153*, 146–157. **DOI:** https://doi.org/10.1007/s00221-003-1588-0, **PMID:** 14610633

Rolls, E. T. (1996). A theory of hippocampal function in memory. *Hippocampus*, *6*, 601–620. **DOI:** https://doi.org/10.1002/(SICI)1098-1063(1996)6:6<601::AID-HIPO5>3.0.CO;2-J, **PMID:** 9034849

Sassenhagen, J., & Draschkow, D. (2019). Cluster-based permutation tests of MEG/EEG data do not establish significance of effect latency or location. *Psychophysiology*, *56*, e13335. **DOI:** https://doi.org/10.1111/psyp.13335, **PMID:** 30657176

Seghier, M. L., & Price, C. J. (2018). Interpreting and utilising intersubject variability in brain function. *Trends in Cognitive Sciences*, *22*, 517–530. **DOI:** https://doi.org/10.1016/j.tics.2018.03.003, **PMID:** 29609894, **PMCID:** PMC5962820

Siegel, M., Warden, M. R., & Miller, E. K. (2009). Phase-dependent neuronal coding of objects in short-term memory. *Proceedings of the National Academy of Sciences, U.S.A.*, *106*, 21341–21346. **DOI:** https://doi.org/10.1073/pnas.0908193106, **PMID:** 19926847, **PMCID:** PMC2779828

Stoet, G., & Hommel, B. (1999). Action planning and the temporal binding of response codes. *Journal of Experimental Psychology: Human Perception and Performance*, *25*, 1625–1640. **DOI:** https://doi.org/10.1037/0096-1523.25.6.1625

Takacs, A., Mückschel, M., Roessner, V., & Beste, C. (2020). Decoding stimulus–response representations and their stability using EEG-based multivariate pattern analysis. *Cerebral Cortex Communications*, *1*, tgaa016. **DOI:** https://doi.org/10.1093/texcom/tgaa01

Takacs, A., Zink, N., Wolff, N., Münchau, A., Mückschel, M., & Beste, C. (2020). Connecting EEG signal decomposition and response selection processes using the theory of event coding framework. *Human Brain Mapping*, *41*, 2862–2877. **DOI:** https://doi.org/10.1002/hbm.24983, **PMID:** 32150315, **PMCID:** PMC7294061

Waschke, L., Kloosterman, N. A., Obleser, J., & Garrett, D. D. (2021). Behavior needs neural variability. *Neuron*, *109*, 751–766. **DOI:** https://doi.org/10.1016/j.neuron.2021.01.023, **PMID:** 33596406